Chemical Science

Conjugated Oligomers Incorporating Azulene Building Blocks – Seven- vs Five-Membered Ring Connectivity

Journal:	*Chemical Science*
Manuscript ID:	SC-EDG-07-2014-002210
Article Type:	Edge Article
Date Submitted by the Author:	24-Jul-2014

Complete List of Authors:	Hawker, Craig; University of California, Materials Research Laboratory Amir, Elizabeth; Shenkar Institute of Technology, Chemistry Chabinyc, Michael L. ; University of California, Santa Barbara, Materials Department Murai, Masahito; Okayama University, Division of Chemistry and Biochemistry Amir, Roey; University of Tel Aviv, Chemistry Cowart, John; University of California, Santa Barbara, Materials Department

Journal Name

RSCPublishing

ARTICLE

Conjugated Oligomers Incorporating Azulene Building Blocks – Seven- vs Five-Membered Ring Connectivity†

Cite this: DOI: 10.1039/xoxxoooooox

Received ooth January 2012,
Accepted ooth January 2012

DOI: 10.1039/xoxxoooooox

www.rsc.org/

Elizabeth Amir,*[a] Masahito Murai,[b] Roey J. Amir,[c] John S. Cowart Jr.,[b] Michael L. Chabinyc [b] and Craig J. Hawker *[b]

The properties of isomeric azulene derivatives based on 7- versus 5-membered ring substitution were examined by the synthesis and characterization of well-defined electroactive oligomers. The substitution pattern was shown to dramatically influence solid-state, electronic and optical properties of the oligomers with acid-responsive materials only being observed when the azulenium cation could be directly stabilized by substituents in the 7-membered ring. Protonation was accompanied by a reversible color change and a strong red-shift of the absorption maximum as indicated by UV-vis studies. In addition, we show that the absorption maxima and optical band-gaps of azulenium cations can be tuned by the nature of the chromophore connected to the seven-membered ring of the azulene nucleus.

Introduction

Functional materials with optical, conductive, and electron-transfer properties are gaining increasing importance due to their potential applications in microelectronics, sensors and energy generation. To facilitate these applications, significant work has been devoted to the design and synthesis of multi-component π-conjugated systems whose electronic properties can be reversibly altered upon external stimuli.[1] Azulenes, which show unique photophysical and electrical properties that are derived from their unusual dipolar and π-electron polarization, represent ideal building blocks for these stimuli-responsive systems.[2-4] For small molecules composed of only C and H, azulenes are noteworthy for their deep blue color and dipole moment of 1.08 D which results from the fusion of an electron-deficient seven-membered ring with an electron-rich five-membered ring.[5] This marked asymmetry opens up the possibility of controlling the optical and electronic properties of azulene-containing materials through the substitution patterns of the different 5- and 7-membered azulene rings. In fact, in recent years azulene derivatives have been utilized as functional monomers for construction of conducting polymers,[3,4,6] dye-sensitized solar cells (DSSCs),[7] nonlinear optical (NLO) materials,[8] charge-transfer complexes,[9] and molecular switches.[10] Among conducting polymers, the pH responsiveness of azulene-based materials is unique with protonation taking place at the electron-rich cyclopentadiene ring of azulene, forming an aromatic 6π-electron azulenium cation.[11] This is in direct contrast to traditional backbones based on poly(thiophene) or poly(phenylene) with the closest analogy being polyaniline systems. However unlike polyaniline, considerable opportunities exist to tailor the substitution pattern of the azulene building block leading to tunable optical, electrochemical and electrochromic properties. This promise is tempered by the difficulty of accessing many substitution patterns using traditional synthetic approaches due to elaborate and low-yielding procedures, which in many cases, lack regiochemical control.[12,13] To address this challenge, we recently reported a new strategy for specific functionalization of the seven-membered ring of azulene allowing for controlled incorporation into the backbone of conjugated materials. The optical band gap of these azulene derivatives could be modulated by simple protonation, with fluorescence being "switched on" upon generation of the corresponding azulenium cations.[14] This unusual pH-responsive behavior, and the paucity of known azulene-based materials conjugated through the seven-membered ring of azulene, motivated an exploration of the synthesis and properties of conjugated oligomers based on azulenes and various aromatic chromophores.

We therefore initially examined isomeric azulene-benzothiophene derivatives, **1** and **2**, in order to obtain structure/property relationships related to 7-membered ring connectivity versus traditional 5-membered ring connectivity (Figure 1). In this system, two benzothiophene moieties are attached to the parent azulene nucleus through the novel C4 and C7 substitution pattern in the 7-membered ring or the more

traditional C1 and C3 positions of the 5-membered ring. The influence of 4,7-disubstitution versus 1,3-disubstitution on the solid-state organization, electrochemical and pH-responsive behavior of these new azulene-based materials was studied with X-ray diffraction analysis, UV-vis spectroscopy, fluorescence, theoretical calculations, electrochemistry and EPR (electron paramagnetic resonance) measurements. In addition, tuning of the absorption maxima and optical band-gaps of the azulenium cations was demonstrated by the preparation of a series of azulene derivatives substituted by various aromatic chromophores through the C4 and C7 positions.

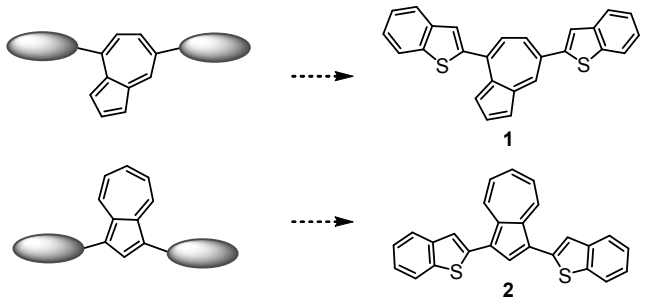

Fig. 1 Novel 7-membered ring connectivity (top) versus traditional 5-membered ring connectivity (bottom) for isomeric azulene derivatives 1 and 2 respectively.

Results and discussion

The synthetic strategy for the isomeric oligoazulenes **1** and **2** is shown in Scheme 1. For conjugation through the 7-membered ring, 4,7-dibromoazulene **3** was prepared via regioselective cycloaddition between dimethylaminofulvene and 2,5-dibromothiophene-*S*,*S*-dioxide as detailed previousely.[14] In contrast, 1,3-dibromoazulene **4**, was prepared by radical bromination of the unsubstituted azulene with *N*-bromosuccinimide (NBS).[15] The isomeric, dibromo-functionalized azulenes **3** and **4** were then independently cross-coupled with benzothiophen-2-trimethylstannane **5** utilizing microwave-assisted Stille cross-coupling at 150 °C for 45 minutes. Precipitation of the crude solutions in methanol, followed by purification gave 4,7-bis(benzo[*b*]thiophene-2-yl)azulene **1** and 1,3-bis(benzo[*b*]thiophene-2-yl)azulene **2** as blue solids in 82% and 86% yields respectively.

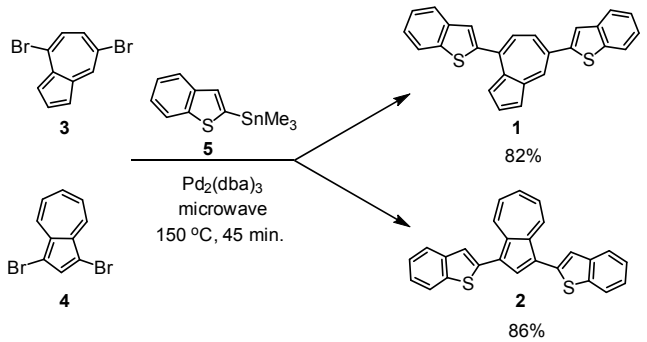

Scheme 1 Synthetic routes to isomeric bis(benzothiophene) azulenes 1 and 2.

X-Ray diffraction analysis of **1** and **2** confirmed incorporation of benzothiophene groups into the targeted positions of the seven- and five-membered rings of azulene with **1** and **2** crystallizing in monoclinic systems with *P*21/*c* and *P*21/*n* space groups, respectively (Figure 2).[16] Significantly, examination of the crystal packing of **1** and **2** revealed two distinctly different packing motifs. Oligomer **1** shows a π-π stacking arrangement between the azulene rings and also between the benzothiophene chromophores in adjacent molecules. In this packing motif, seven- and five-membered rings of one azulene molecule overlap with seven- and five-membered rings of the adjacent azulene molecule with an average intermolecular distance of 3.9 Å. In contrast, isomer **2** adopts a reverse packing arrangement of the seven-membered rings for the azulene units in adjacent molecules with the five-membered rings bearing the benzothiophene substituents pointing in opposite directions. This difference in solid-state organization for the isomers **1** and **2** clearly demonstrates the influence of substitution pattern on molecular packing which is expected to significantly impact transport and other physical properties.

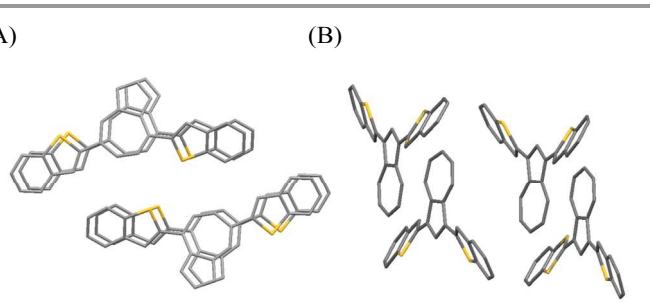

Fig.2 Solid-state packing of isomeric azulenes **1** (A) and **2** (B).

Initial studies on the influence of regiochemistry on the physical properties of these azulene derivatives involved electrochemical measurements. For isomer **1**, conjugated through the 7-membered ring, only a single, irreversible reduction wave in the range -1.62 to -2.19 V under cathodic sweep and no detectable oxidation wave was observed. In comparison, the electrochemical behavior of **2** was essentially the opposite, revealing only an oxidation wave (Figure 3). A rationale for this clear difference is that electron removal occurs at the electron-rich, 5-membered ring to form a radical cation, which is unstable in the absence of substituents in the cyclopentadiene ring. As a result, no oxidation peak is observed for **1**. In fact, this hypothesis was further supported by theoretical calculations as the plots of the HOMOs for compounds **1** and **2** show that electron density lies primarily on the 5-membered ring of azulene (Figure 5). In addition, a well-resolved symmetric EPR signal was only observed for the 1,3-disubstituted azulene **2** upon chemical oxidation with TFA (*g*-factor value = 2.0020, peak-to-peak line width (Δ*H*) = 11.63 G).

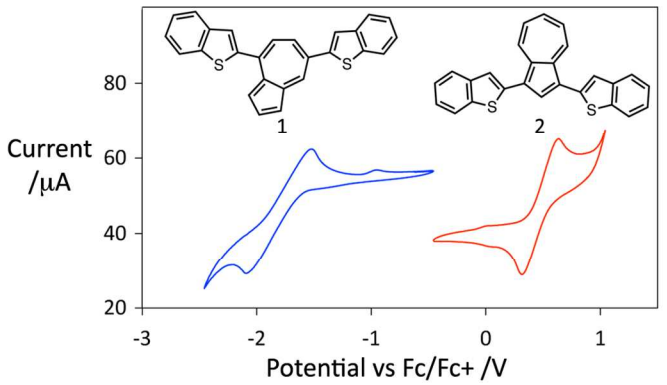

Fig. 3 Cyclic voltammograms of the 7- and 5-membered ring substituted isomeric azulenes **1** and **2**.

To further understand the influence of substitution pattern on the properties and stability of the isomeric azulene derivatives, examination of the UV-vis spectra in the presence or absence of acid offers a direct insight into the extent of conjugation, π-π* transitions and the stability to acid doping for **1** and **2**. In the neutral state, both compounds exhibit spectral profiles with major absorption bands at 320 and 410 nm (band at 410 nm is much stronger for **1**) and one weak absorption band at 630 nm due to the S_0 - S_1 transition of the azulene unit (Figure 4). Upon addition of trifluoroacetic acid (TFA) to the dichloromethane solution of **2**, no new absorption bands were detected with only a decrease in intensity being observed with time. In contrast, protonation of **1** resulted in the disappearance of all the original bands and the formation of a significant, new peak at 536 nm, which can be attributed to the corresponding azulenium cation **1-H**$^+$.[17] This process was accompanied by an instant color change of the solution from deep-blue to orange-red with the absorption maximum of the azulenium cation **1-H**$^+$ being red-shifted by more than 100 nm. Formation of azulenium cation was shown to be a reversible process with the addition of base (triethylamine) regenerating neutral **1** and the original absorption bands. Significantly, protonation-deprotonation could be repeated over many cycles with no observed degradation, demonstrating stabilization of the tropylium cation through conjugation with the benzothiophene rings at the 4- and 7-positions. In contrast, neutralization of acidic solutions of **2** did not recover the original UV-vis spectra, presumably due to decomposition of the unstable protonated azulene species which lacks substitution in the 7-membered ring.[3i]

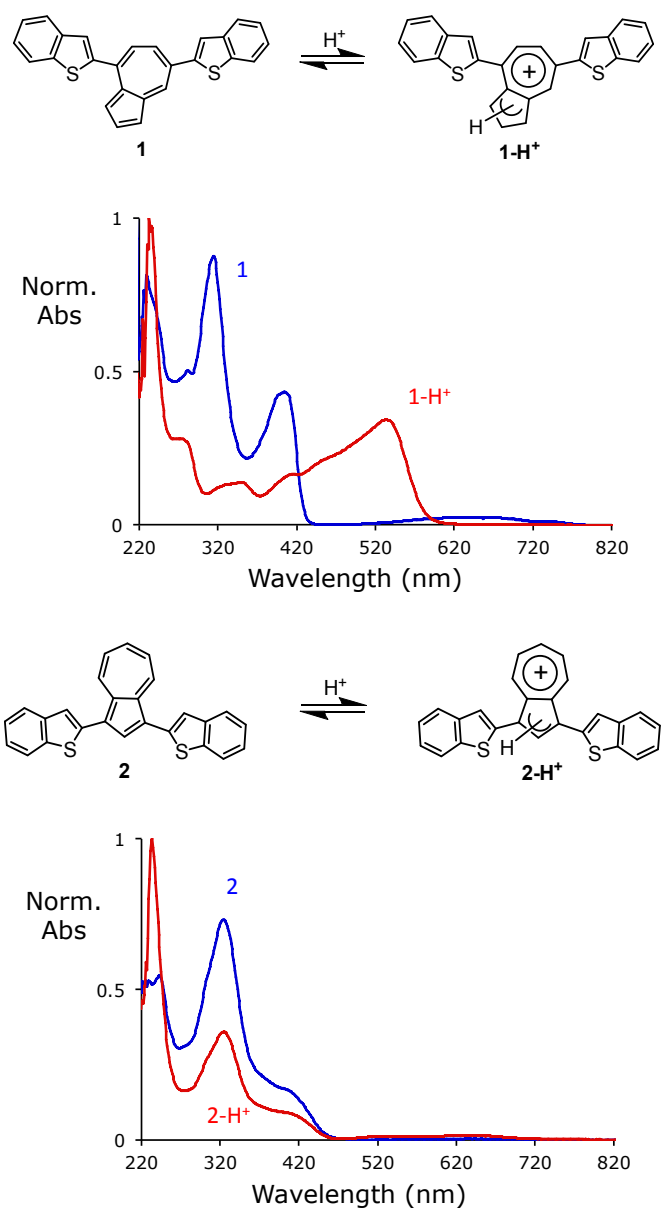

Fig. 4 UV-vis spectra of 4,7-bis(benzothiophene)azulene (**1**) and 1,3-bis(benzothiophene)azulene (**2**) before (shown in blue) and after (shown in red) protonation with TFA.

In order to gain insight into the significantly different stimuli-responsive properties of these substituted azulene derivatives, molecular orbital (MO) calculations for **1** and **2** in the neutral and protonated states were carried out using the B3LYP functional with 6-31+G* basis sets. The optimized structures of **1** and **2** in the neutral states are in good agreement with the corresponding crystal structures and the calculated HOMO and LUMO energy levels for these compounds were found to have comparable values (Figure 5). It is noteworthy that protonation of azulene units leads to changes in the distribution of HOMO/LUMO orbitals. For the cationic states of both **1-H**$^+$ and **2-H**$^+$, the azulene core dominates the LUMO, whereas one of the benzothiophene units primarily contributes to the HOMO. In addition, MO coefficients are delocalized

over the majority of the molecule for the LUMO of **1-H**$^+$, while the corresponding LUMO of **2-H**$^+$ localizes only on the azulene ring indicating stronger conjugation in **1-H**$^+$ than **2-H**$^+$. These differences are primarily derived from the molecular twist between the azulene core and benzothiophene units, which reduces conjugation leading to higher LUMO and lower HOMO levels for **2-H**$^+$ compared with **1-H**$^+$. These observations are in accordance with the red-shift of the lowest energy absorption band for **1** upon the addition of TFA, which was not observed for **2**.

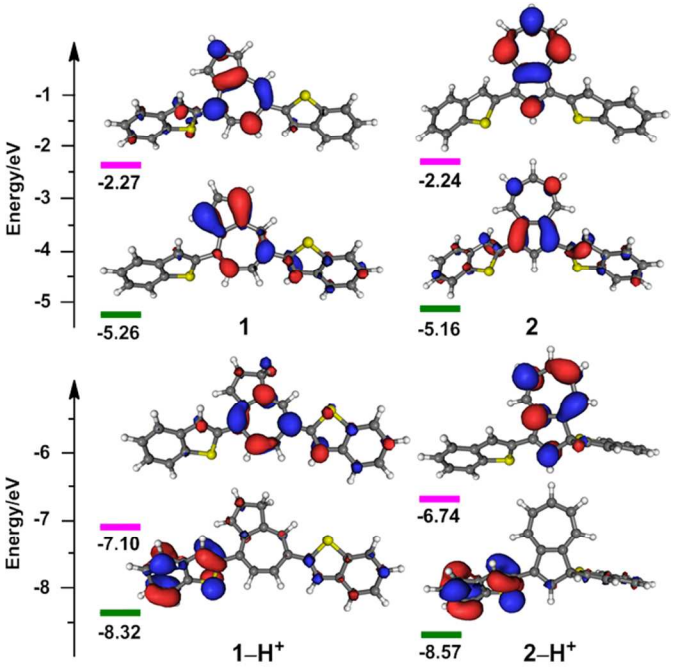

Fig. 5 Energy-level diagrams for the frontier MOs and their contour plots for compounds **1** and **2** in neutral and cationic states. The nodal patterns of each MO are shown at an isosurface value of 0.03 a.u.

The above results demonstrate the importance of the substitution pattern for azulene-based materials and their influence on physical properties such as doping/protonation where stable formation of the 6π-electron tropylium cations is significantly favored by substituents directly attached to the 7-membered ring of the azulene nucleus. To demonstrate the versatility of our synthetic approach and the ability to tune optical properties of azulene-containing materials, a series of conjugated oligomers with various aromatic substituents attached to the seven-membered ring of azulene was examined (Scheme 2). Cross-coupling of 4,7-dibromoazulene **3** or 4,7-dibromo-6-dodecylazulene **6** with aromatic trimethylstannyl derivatives **7-10** under the conditions described above, resulted in the formation of the novel azulene derivatives **11-14** substituted at the C4 and C7 positions with either phenyl, furan, *N*-methylpyrrole or bis(thiophene) rings in high yields (Scheme 2).

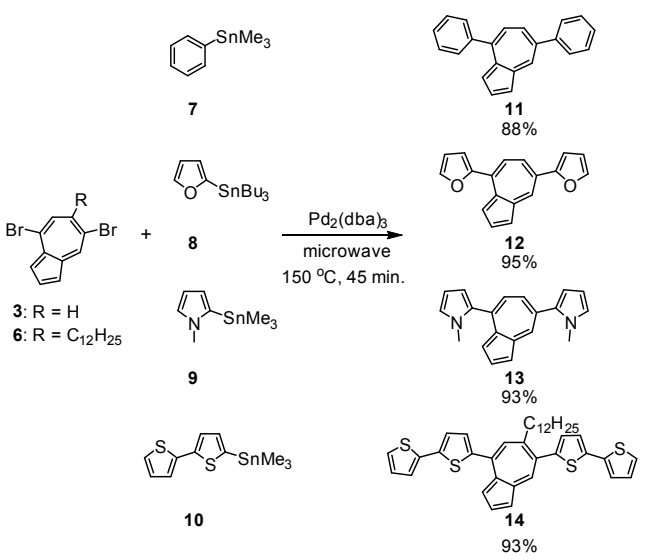

Scheme 2 Synthesis of 4,7-disubstituted azulenes 11 - 14 functionalized via the 7-membered ring.

Fluorescence studies of oligoazulenes **1**, **2**, **11** - **14** in dichloromethane revealed that all the compounds are essentially nonfluorescent in their neutral state similar to the unsubstituted azulene, which has an extremely weak S_1 - S_0 fluorescence.[18] While protonation with TFA had no effect on the fluorescence of **1**, **2**, **11**, **13** and **14**, fluorescence of the azulenium cation derived from 4,7-(bisfuran)azulene (**12**) was "switched on" accompanied by a strong emission band at λ_{max} = 547 nm, Φ_f = 0.154. Fluorescence of the azulenium cation **12-H**$^+$ can be "switched off" by a subsequent addition of base such as triethylamine.

Similar to compound **1**, formation of azulenium cations upon addition of TFA to dichloromethane solutions of **11-14** was accompanied by the appearance of new peaks in the UV-vis spectra (Figure 6). In all cases, the absorption maxima were red-shifted relative to the original π-π* transitions indicating narrowing of the optical band-gap and efficient conjugation of the azulenium cation with the adjacent aromatic rings.[19] Furthermore, the nature of the conjugated substituent incorporated through the seven-membered ring of the parent azulene building block allowed tuning of the absorption maximum of the corresponding azulenium cation. For the azulenium cation **11-H**$^+$, substituted with two phenyl groups, only a minor shift in the λ_{max} to 404 nm was observed, while the absorption maximum of **12-H**$^+$ bearing two furyl groups was considerably higher (λ_{max} = 504 nm). The presence of *N*-methylpyrrole and bis(thiophene) substituents resulted in the most dramatic impact on the absorption maxima of the corresponding azulenium cations with λ_{max} = 567 nm and λ_{max} = 591 nm for **13-H**$^+$ and **14-H**$^+$, respectively. Significantly, in all cases the original absorption spectra of compounds **11-14** were regenerated upon neutralization of the acidic solution with triethylamine, demonstrating that this reversibility is an inherent feature of azulene derivatives substituted in the 7-membered ring.

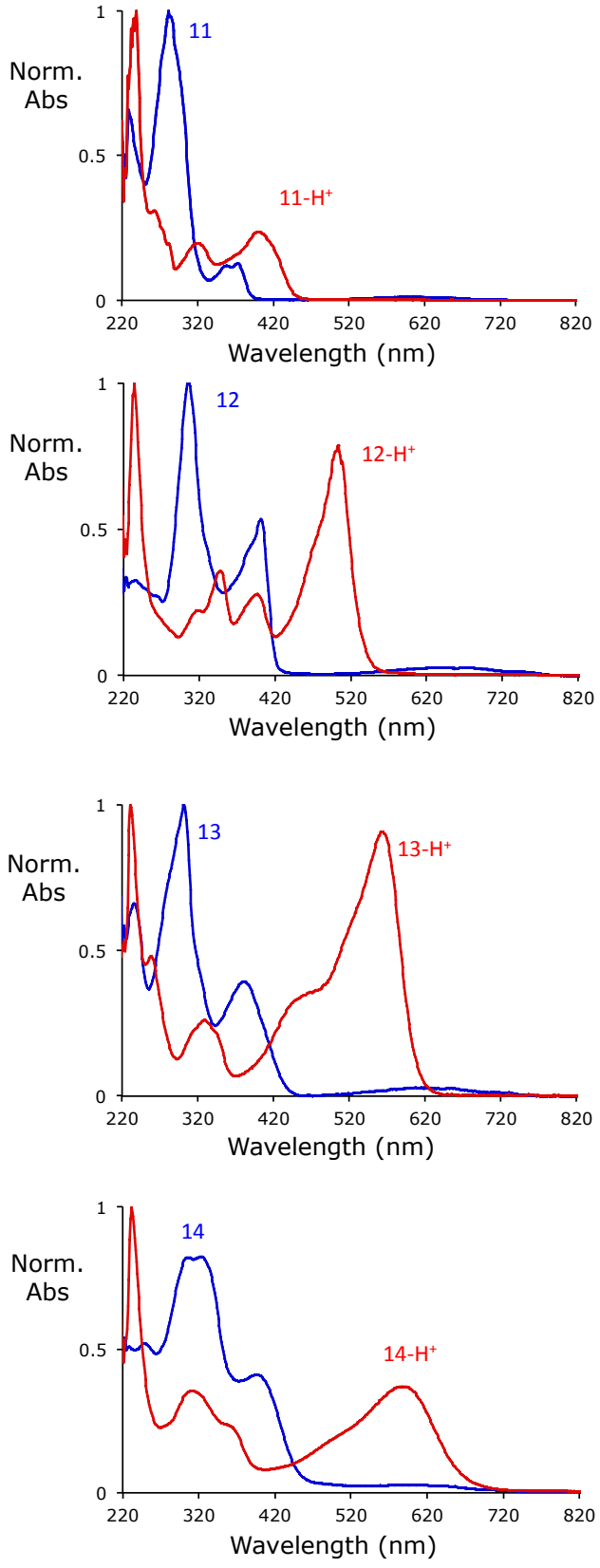

Fig. 6 UV-vis spectra of the oligoazulenes **11** - **14** before (shown in blue) after (shown in red) protonation with TFA.

Conclusions

We have synthesized a new family of azulene-based materials conjugated with various aromatic chromophores through the seven-membered ring of azulene. This non-traditional connectivity results in distinctive solid-state organization and electrochemical behavior when compared with isomeric azulene derivatives having the standard five-membered ring substitution pattern. These results also indicate that covalent attachment of aromatic units to the seven-membered azulene ring is essential for stabilization of the corresponding azulenium cation, which can be generated in a reversible process upon protonation and the absorption maximum and optical band-gap of the azulenium cation can be tuned by the nature of the substituents. We are currently developing strategies to incorporate these new azulene derivatives as electroactive units into polymeric systems and expand the study of stimuli-responsive materials for electronic and photovoltaic applications.

Experimental

2,2'-(azulene-4,7-diyl)dibenzo[*b*]thiophene (1) was prepared from 4,7-dibromoazulene (**3**) and benzo[*b*]thiophene-2-yltrimethylstannane (**5**) in 82% yield. A 5 mL glass vial was charged with a stirrer bar, 0.2 mmol of azulene **3**, 0.5 mmol of **6**, $Pd_2(dba)_3$ (4 mol% Pd), P(*o*-tol)$_3$ (8 mol%) and chlorobenzene (2 mL). The glass vial was purged with nitrogen and securely sealed. The glass vial was placed into a microwave reactor and heated at 150 ^oC for 45 minutes with stirring. After cooling to room temperature, the solvent was evaporated and the crude product was purified using column chromatography, eluting with hexanes/dichloromethane (1:1). ^1H NMR (600 MHz, $CDCl_3$, ppm): δ 8.86 (1H, d, J = 2 Hz), 8.06 (1H, dd, J_1 = 11 Hz, J_2 = 2 Hz), 7.92-7.91 (2H, m), 7.88 (1H, dd, J_1 = 7 Hz, J_2 = 1 Hz), 7.85 (1H, d, J = 8 Hz), 7.81 (1H, d, J = 8 Hz), 7.76 (1H, s), 7.70 (1H, d, J = 4 Hz), 7.66 (1H, s), 7.57 (1H, dd, J_1 = 4 Hz, J_2 = 1 Hz), 7.49 (1H, d, J = 11 Hz), 7.44-7.33 (4H, m). ^{13}C NMR (125 MHz, $CDCl_3$, ppm): δ 147.0, 144.5, 141.6, 140.9, 140.3, 140.2, 139.8, 139.6, 138.1, 136.8, 136.2, 134.3, 127.9, 125.6, 125.0, 124.9, 124.74, 124.68, 124.5, 124.1 123.6, 123.4, 122.24, 122.19, 120.5, 120.0. HRMS (FI) (*m*/*z*): $(M)^+$ calcd for $C_{26}H_{16}S_2$ 392.0693; found, 392.0689.

1,3-di(benzo[*b*]thiophen-2-yl)azulene (2) was prepared from 1,3-dibromoazulene (**4**) and benzo[*b*]thiophene-2-yltrimethylstannane (**5**) as described above in 86% yield. ^1H NMR (400 MHz, $CDCl_3$, ppm): δ 8.88 (2H, d, J = 10 Hz), 8.33 (1H, s), 7.89 (2H, d, J = 8 Hz), 7.84 (2H, d, J = 8 Hz), 7.69 (1H, t, J = 10 Hz), 7.53 (2H, s), 7.42 - 7.28 (6H, m). ^{13}C NMR (100 MHz, $CDCl_3$, ppm): δ 140.8, 140.2, 140.0, 139.0, 138.0, 136.9, 125.3, 124.6, 124.1, 123.4, 123.3, 122.2, 121.4. HRMS (FI) (*m*/*z*): $(M)^+$ calcd for $C_{26}H_{16}S_2$ 392.0693; found, 392.0680.

4,7-diphenylazulene (11) was prepared from 4,7-dibromoazulene (**3**) and trimethyl(phenyl)stannane (**7**) as described above in 88% yield. ^{1}H NMR (600 MHz, $CDCl_3$, ppm): δ 8.71 (1H, d, J = 2 Hz), 7.89 - 7.85 (2H, m), 7.70 - 7.65 (3H, m), 7.53 - 7.46 (4H, m), 7.40 (1H, t, J = 7 Hz), 7.29 - 7.22 (2H, m), 7.17 (1H, d, J = 7 Hz), 7.08 (1H, t, J = 7 Hz), 6.74 - 6.72 (1H, m). ^{13}C NMR (125 MHz, $CDCl_3$, ppm): δ 149.3, 144.5, 143.4, 140.5, 137.9, 137.3, 136.8, 136.5, 134.9, 133.0, 130.1, 129.2, 128.8, 128.7, 128.2, 128.1, 128.0, 127.0, 126.1, 125.4, 120.4, 118.6. HRMS (FI) (m/z): $(M)^+$ calcd for $C_{22}H_{16}$ 280.1252; found, 280.1246.

2,2'-(azulene-4,7-diyl)difuran (12) was prepared from 4,7-dibromoazulene (**3**) and tributyl(furan-2-yl)stannane (**8**) as described above in 95% yield. ^{1}H NMR (400 MHz, $CDCl_3$, ppm): δ 8.80 (1H, d, J = 2 Hz), 8.08 (1H, dd, J_1 = 11 Hz, J_2 = 2 Hz), 7.87 (1H, t, J = 4 Hz), 7.84 - 7.83 (1H, m), 7.70 (1H, d, J = 2 Hz), 7.66 (1H, d, J = 11 Hz), 7.55 (1H, d, J = 2 Hz), 7.47 (1H, dd, J_1 = 4 Hz, J_2 = 1 Hz), 7.11 (1H, d, J = 4 Hz), 6.79 (1H, d, J = 3 Hz), 6.65 (1H, dd, J_1 = 3 Hz, J_2 = 2 Hz), 6.55 (1H, dd, J_1 = 3 Hz, J_2 = 2 Hz). ^{13}C NMR (100 MHz, $CDCl_3$, ppm): δ 143.8, 142.7, 141.3, 137.6, 135.7, 134.1, 133.3, 131.3, 124.1, 122.6, 121.5, 118.5, 113.1, 112.4, 112.1, 105.8. HRMS (FI) (m/z): $(M)^+$ calcd for $C_{18}H_{12}O_2$ 260.0837; found, 260.0814.

2,2'-(azulene-4,7-diyl)bis(1-methyl-pyrrole) (13) was prepared from 4,7-dibromoazulene (**3**) and 1-methyl-2-(trimethylstannyl)pyrrole (**9**) as described above in 93% yield. ^{1}H NMR (400 MHz, $CDCl_3$, ppm): δ 8.49 (1H, d, J = 2 Hz), 7.86 (1H, t, J = 4 Hz), 7.66 (1H, dd, J_1 = 11 Hz, J_2 = 2 Hz), 7.42 (1H, dd, J_1 = 4 Hz, J_2 = 1 Hz), 7.24 (1H, d, J = 3 Hz), 7.19 (1H, d, J = 11 Hz), 6.84 (1H, t, J = 2 Hz), 6.77 (1H, t, J = 2 Hz), 6.47 (1H, dd, J_1 = 4 Hz, J_2 = 2 Hz), 6.33 - 6.31 (2H, m), 6.26 (1H, t, J = 3 Hz), 3.71 (3H, s), 3.55 (3H, s). ^{13}C NMR (100 MHz, $CDCl_3$, ppm): δ 140.0, 139.5, 138.7, 138.3, 137.1, 136.8, 135.4, 126.6, 125.8, 123.9, 123.7, 120.1, 119.1, 111.3, 109.4, 108.07, 108.06, 35.2, 35.1. HRMS (EI) (m/z): $(M)^+$ calcd for $C_{20}H_{18}N_2$ 286.1470; found, 286.1477.

5,5'-(6-dodecylazulene-4,7-diyl)di-2,2' bithiophene (14) was prepared from 4,7-dibromo-6-dodecylazulene (**6**) and 2,2'-bithiophen-5-yltrimethylstannane (**10**) as described above in 93% yield. ^{1}H NMR (400 MHz, $CDCl_3$, ppm): δ 8.50 (1H, s), 7.83 (1H, t, J = 4 Hz), 7.67 (1H, d, J = 4 Hz), 7.51 (1H, d, J = 4 Hz), 7.45 (1H, s), 7.40 (1H, dd, J_1 = 4 Hz, J_2 = 1 Hz), 7.31 - 7.28 (3H, m), 7.26 - 7.23 (2H, m), 7.19 (1H, d, J = 4 Hz), 7.10 - 7.05 (2H, m), 6.95 (1H, d, J = 4 Hz), 2.89 - 2.85 (2H, m), 1.69 - 1.67 (2H, m), 1.33 - 1.24 (18H, m), 0.90 (3H, t, J = 7 Hz). ^{13}C NMR (100 MHz, $CDCl_3$, ppm): δ 152.0, 145.1, 144.3, 140.9, 138.8, 138.3, 137.5, 137.4, 137.2, 136.5, 134.5, 133.2, 130.22, 130.17, 129.2, 128.8, 128.1, 128.0, 127.3, 126.3, 125.0, 124.5, 124.3, 124.0, 123.8, 123.5, 121.6, 119.2, 40.9, 33.4, 32.1, 29.9, 29.83, 29.81, 29.8 29.7, 29.5, 29.4, 22.9, 14.3. HRMS (FI) (m/z): $(M)^+$ calcd for $C_{38}H_{40}S_4$ 624.2013; found, 624.2006.

Acknowledgements

This work was partially supported by the DOE Basic Energy Science under award DE-SC0005414 (E.A., M.M., and C.J.H.), the NSF PREM program between UCSB and UTEP (DMR-1205302) (J.J.C., M.L.C., and C.J.H.) and the MRSEC Program of the NSF under award no. DMR-1121053 (R.J.A., J.J.C., and C.J.H.).

Notes and references

[a] Shenkar College of Engineering and Design, Department of Plastics Engineering, Ramat-Gan 52526, Israel.
[b] Materials Department, Materials Research Laboratory, and Department of Chemistry & Biochemistry, University of California, Santa Barbara, California 93106.
[c] School of Chemistry, Tel-Aviv University, Tel-Aviv 69978, Israel.

Correspondance: hawker@mrl.ucsb.edu (CJH); eamir@shenkar.ac.il (EA).

† Electronic Supplementary Information (ESI) available: Experimental details, ^{1}H and ^{13}C-NMR spectra of oligoazulenes **1**, **2**, **11-14**, crystal structures of oligoazulenes **1** and **2**, fluorescence and electrochemical studies, EPR measurements and theoretical calculations. See DOI: 10.1039/b000000x/

1 (a) T. M. Swager, *Acc. Chem. Res.*, 1998, **31**, 201-207. (b) R. H. Friend, R. W. Gymer, A. B. Holmes, J. H. Burroughes, R. N. Marks, C. Taliani, D. D. C. Bradley, D. A. Dos Santos, J. L. Brédas, M. Lögdlund and W. R. Salaneck, *Nature*, 1999, **397**, 121-128. (c) D. T. McQuade, A. E. Pullen and T. M. Swager, *Chem. Rev.*, 2000, **100**, 2537-2574. (d) S. Anderson, *Chem.-Eur. J.*, 2001, **7**, 4706-4714. (e) T. Mrozek, J. Daub and A. Ajayaghosh, In *Molecular Switches*; Feringa, B. L., Ed.; Wiley-VCH: Weinheim, Germany, 2001; pp 63-106. (f) T. Gupta and M. E. van der Boom, *J. Am. Chem. Soc.*, 2006, **128**, 8400-8401. (g) A. Rostami and M. S. Taylor, *Macromol. Rapid Commun.* 2012, **33**, 21-34. (h) O. Yarimaga, J. Jaworski, B. Yoon and J.-M. Kim, *Chem. Commun.*, 2012, **48**, 2469-2485. (i) X. Yan, F. Wang, B. Zheng and F. Huang, *Chem. Soc. Rev.*, 2012, **41**, 6042-6065. (j) M. A. Naik and S. Patil, *J. Polym. Sci. Part A; Polym. Chem.* **2013**, *51*, 4241–4260. (k) M. J. Robb, S.-Y. Ku, F. G. Brunetti, C. J. Hawker, *J. Polym. Sci. Part A; Polym. Chem.* **2013**, *51*, 1263-1271.

2 (a) K.-P. Zeller, Azulene. In Houben-Weyl: Methoden der Organischen Chemie, 4th ed.; Georg Thieme: Stuttgart, Germany, 1985; Vol. V, Part 2C, pp 127-418. (b) P. Foggi, F. V. R. Neuwahl, L. Moroni and P. R. Salvi, *J. Phys. Chem.* A, 2003, **107**, 1689-1696. (c) S. V. Shevyakov, H. Li, R. Muthyala, A. E. Asato, J. C. Croney, D. M. Jameson and R. S. H. Liu, *J. Phys. Chem.* A, 2003, **107**, 3295-3299. (d) A. L. Crombie, J. L. Kane, K. M. Shea and R. L. Danheiser, *J. Org. Chem.*, 2004, **69**, 8652-8667. (e) M. Koch, O. Blacque and K. Venkatesan, *Org. Lett.*, 2012, **14**, 1580-1583.

3 (a) G. Tourillon and F. Garnier, *J. Electroanal. Chem.*, 1982, **135**, 173-178. (b) M. Iyoda, K. Sato and M. Oda, *Tetrahedron Lett.*, 1985,

26, 3829-3832. (c) R. J. Waltman and J. Bargon, *Can. J. Chem*., 1986, **64**, 76-95. (d) K. G. Neoh, E. T. Kang and T. C. Tang, *Polym. Bull*., 1988, **19**, 325-331. (e) J. Daub, M. Feuerer, A. Mirlach and J. Salbeck, *Synth. Met*., 1991, **42**, 1551-1555. (f) W. Schuhmann, J. Huber, A. Mirlach and J. Daub, *Adv. Mater*., 1993, **5**, 124-126. (g) M. Porsch, G. Sigl-Seifert and J. Daub, *Adv. Mater*., 1997, **9**, 635-639. (h) F. X. Redl, O. Köthe, K. Röckl, W. Bauer and J. Daub, *Macromol. Chem. Phys*., 2000, **201**, 2091-2100. (i) F. Wang, Y.-H. Lai, N. M. Kocherginsky and Y. Y. Koteski, *Org. Lett*., 2003, **5**, 995-998. (j) B. Meana-Esteban, C. Lete, C. Kvarnstroem and A. Ivaska, *J. Phys. Chem*. B, 2006, **110**, 23343-23350. (k) G. Nie, T. Cai, S. Zhang, J. Hou, J. Xu and X. Han, *Mater. Lett*., 2007, **61**, 3079-3082.

4 (a) S. E. Estdale, R. Brettle, D. A. Dummur and C. M. Marson, *J. Mater. Chem*., 1997, **7**, 391-401. (b) Z. Hussain, H. Hopf, L. Pohl, T. Oeser, A. K. Fischer and P. G. Jones, *Eur. J. Org. Chem*., 2006, 5555-5569. (c) F. Wang and Y.-H. Lai, *Macromolecules*, 2003, **36**, 536-538. (d) F. Wang, Y.-H. Lai and M.-Y. Han, *Org. Lett*., 2003, **5**, 4791-4794. (e) F. Wang, Y.-H. Lai and M.-Y. Han, *Macromolecules*, 2004, **37**, 3222-3230. (f) X. Wang, J.-K. Ng, P. Jia, T. Lin, C. M. Cho, J. Xu, X. Lu and C. He, *Macromolecules*, 2009, **42**, 5534-5544. (g) J. Xia, B. Capozzi, S. Wei, M. Strange, A. Batra, J. R. Moreno, R. J. Amir, E. Amir, G. C. Solomon, L. Venkataraman and L. M. Campos, *Nano Lett*., 2014, **14**, 2941-2945.

5 A. St. Pfau and P. A. Plattner, *Helv. Chim. Acta*, 1939, **22**, 202-208.

6 For polyazulenes connected via seven-membered ring: M. Murai, E. Amir, R. J. Amir and C. J. Hawker, *Chem. Sci*., 2012, **3**, 2721-2725.

7 X.-H. Zhang, C. Li, W.-B. Wang, X.-X. Cheng, X.-S. Wang and B.-W. Zhang, *J. Mater. Chem*., 2007, **17**, 642-649.

8 (a) C. Lambert, G. Nöll, M. Zabel, F. Hampel, E. Schmälzlin, C. Bräuchle and K. Meerholz, *Chem. Eur., J*., 2003, **9**, 4232-4239. (b) L. Cristian, I. Sasaki, P. G. Lacroix, B. Donnadieu, I. Asselberghs, K. Clays and A. C. Razus, *Chem. Mater*., 2004, **16**, 3543-3551.

9 (a) S. Schmitt, M. Baumgarten, J. Simon and K. Hafner, *Angew. Chem., Int. Ed*., 1998, **37**, 1077-1081. (b) J. E. Frey, A. M. Andrews, S. D. Combs, S. P. Edens, J. J. Puckett, R. E. Seagle and L. A. Torreano, *J. Org. Chem*., 1992, **57**, 6460-6466.

10 (a) T. Mrozek, H. Görner and J. Daub, *Chem. Eur. J*., 2001, **7**, 1028-1040. (b) M. Koch, O. Blacque and K. Venkatesan, *J. Mater. Chem*. C, 2013, **1**, 7400-7408. (c) T. Tang, T. Lin, F. Wang and C. He, *Polym. Chem*., 2014, **5**, 2980-2989.

11 K. H. Grellmann, E. Heilbronner, P. Seiler and A. Weller, *J. Am. Chem. Soc*., 1968, **90**, 4238-4242.

12 S. Carret, A. Blanc, Y. Coquerel, M. Berthod, A. E. Greene and J.-P. Deprés, *Angew. Chem., Int. Ed*., 2005, **44**, 5130-5133.

13 A. L. Crombie, J. L. Kane, Jr., K. M. Shea and R. L. Danheiser, *J. Org. Chem*., 2004, **69**, 8652-8667.

14 E. Amir, R. J. Amir, L. M. Campos and C. J. Hawker, *J. Am. Chem. Soc*., 2011, **133**, 10046-10049.

15 F. Wang, Y.-H. Lai, N. M. Kocherginsky and Y. Y. Kosteski, *Org. Lett*., 2003, **5**, 995-998.

16 Crystal structures of **1** and **2** are shown in the SI. Crystal structures were deposited at the Cambridge Crystallographic Data Centre (CCDC) and the data have been assigned the following deposition numbers: CCDC 943616 (compound **1**) and CCDC 943617 (compound **2**).

17 (a) P. A. Plattner, E. Heilbronner and S. Weber, *Helv. Chim. Acta*, 1952, **35**, 1036-1049. (b) M. Oda, A. Fukuta, T. Kajioka, T. Uchiyama, H. Kainuma, R. Miyatake and S. Kuroda, *Tetrahedron*, 2000, **56**, 9917-9925. (c) S.-L. Chen, R. Klein and K. Hafner, *Eur. J. Org. Chem*., 1998, 423-433.

18 (a) M. Beer and H. C. Longuet-Higgins, *J. Chem. Phys*., 1955, **23**, 1390-1391. (b) P. M. Rentzepis, *Chem. Phys. Lett*. 1969, **3**, 717-720.

19 The optical band gaps of the azulenium cations $\mathbf{11}^{+}$-$\mathbf{14}^{+}$, estimated by the onset point of the absorption bands, can be found in the SI.

TOC:

Conjugated Oligomers Incorporating Azulene Building Blocks – Seven- vs Five-Membered Ring Connectivity†

Elizabeth Amir,* Masahito Murai, Roey J. Amir, John S. Cowart Jr., Michael L. Chabinyc and Craig J. Hawker*